ACTA ONCOLOGICA, 2017
VOL. 56, NO. 6, 832–838
http://dx.doi.org/10.1080/0284186X.2017.1297536

Taylor & Francis
Taylor & Francis Group

ORIGINAL ARTICLE

Comparison of gastric-cancer radiotherapy performed with volumetric modulated arc therapy or single-field uniform-dose proton therapy

Gracinda Mondlane[a,b], Michael Gubanski[c], Pehr A. Lind[c,d], Ana Ureba[a] and Albert Siegbahn[a]

[a]Department of Physics – Medical Radiation Physics, Stockholm University, Stockholm, Sweden; [b]Department of Physics, Universidade Eduardo Mondlane, Maputo, Mozambique; [c]Department of Oncology and Pathology, Karolinska University Hospital, Stockholm, Sweden; [d]Department of Oncology, Södersjukhuset, Stockholm, Sweden

ABSTRACT

Background: Proton-beam therapy of large abdominal cancers has been questioned due to the large variations in tissue density in the abdomen. The aim of this study was to evaluate the importance of these variations for the dose distributions produced in adjuvant radiotherapy of gastric cancer (GC), implemented with photon-based volumetric modulated arc therapy (VMAT) or with proton-beam single-field uniform-dose (SFUD) method.

Material and methods: Eight GC patients were included in this study. For each patient, a VMAT- and an SFUD-plan were created. The prescription dose was 45 Gy (IsoE) given in 25 fractions. The plans were prepared on the original CT studies and the doses were thereafter recalculated on two modified CT studies (one with extra water filling and the other with expanded abdominal air-cavity volumes).

Results: Compared to the original VMAT plans, the SFUD plans resulted in reduced median values for the V18 of the left kidney (26%), the liver mean dose (14.8 Gy (IsoE)) and the maximum dose given to the spinal cord (26.6 Gy (IsoE)). However, the PTV coverage decreased when the SFUD plans were recalculated on CT sets with extra air- (86%) and water-filling (87%). The added water filling only led to minor dosimetric changes for the OARs, but the extra air caused significant increases of the median values of V18 for the right and left kidneys (10% and 12%, respectively) and of V10 for the liver (12%). The density changes influenced the dose distributions in the VMAT plans to a minor extent.

Conclusions: SFUD was found to be superior to VMAT for the plans prepared on the original CT sets. However, SFUD was inferior to VMAT for the modified CT sets.

ARTICLE HISTORY
Received 3 February 2017
Accepted 16 February 2017

KEYWORDS
Gastric cancer; radiotherapy; scanned-proton beams; density variations; dosimetric comparison

Introduction

Gastric cancer (GC) is the fifth most common cancer type and the third leading cause of death from cancer worldwide [1]. Despite the fact that the incidence has decreased in developed countries in recent years, the majority of GC patients will present locally-advanced or metastatic disease. Surgery is still considered the most effective treatment of GC [2–4]. However, since most GC patients are diagnosed in an advanced stage, the prognosis is poor. Other treatments, including radiotherapy (RT) and chemotherapy, have attracted increased interest in recent years. Regarding the combination of these two treatments, the role of chemoradiotherapy for the treatment of GC has been addressed in different clinical trials, e.g., the SWOG-directed Intergroup 0116 trial [5] and the British MAGIC trial [6]. In the former study, an increase in the overall survival of 9 months was reported. Based on the results of this study, postoperative chemoradiotherapy has become the standard treatment of GC in the United States [7]. In the latter study, an increase of 13% in the 5-year survival rate was obtained for perioperative chemotherapy. These results showed the potential gain of adding other oncological treatments to surgery and inspired on-going trials, e.g., the European CRITICS trial (clinicaltrials.gov NCT00407186) [8] and the Australian TOPGEAR trial (clinicaltrials.gov NCT01924819).

When proton beam therapy (PBT) is used for the treatment of certain abdominal- and pelvic-cancers, the doses given to the organs at risk (OAR) can be reduced, while offering a similar dose coverage to the planning target volume (PTV), compared to photon-beam based RT [4,9–12]. In the majority of these studies, the proton plans were prepared for irradiation with the passive-scattering technique. Some doubts have been raised against the proposition of treating targets in the vicinity of the bowels with protons, in particular with the active scanning technique, due to the unpredictable bowel movement and the variations in the bowel-gas content. Due to the high sensitivity of the proton-beam range to tissue-density variations, the calculated dose at the proximal and distal edge of intra-abdominal PTVs becomes unreliable. These dosimetric uncertainties have been commented, but not quantified, in previously published studies on this topic [12,13].

CONTACT Gracinda Mondlane gracinda.mondlane@fysik.su.se Department of Medical Radiation Physics, Stockholm University, Box 260, 171 76 Stockholm, Sweden

Supplemental data for this article can be accessed here.

The aim of this study was to quantify the impact of large variations in gastrointestinal gas filling on the dose distributions produced in photon-beam based volumetric modulated arc therapy (VMAT) and in proton-beam based single-field uniform-dose (SFUD) treatments of GC patients. The density variations were studied by simulating two worst-case scenarios. In one of these cases, the abdominal gas was replaced by water-equivalent material. In the other case, the abdominal air cavities were enlarged by 5 mm in all directions.

Material and methods

Patients and delineation of structures

Eight consecutive patients planned for adjuvant treatment within the CRITICS trial at the Radiotherapy Department at Karolinska University Hospital, were selected for this study. The patients had undergone partial (seven patients) or total (one patient) gastrectomy prior to the acquisition of the planning CT-scan. The median age of the patients was 60 years (range 41–68 years). All patients had acceptable kidney function in both kidneys according to the preoperative kidney scintigraphy and adequate liver function on hematological evaluation. They had nutrition support either by a nasogastric tube or nutritive jejunostoma. The patients signed an informed written consent prior to enrollment. The study protocol was approved by the Ethics Committee at the Karolinska Institute and by the Radiation Protection Committee at *Södersjukhuset* Hospital in Stockholm.

Recommendations for target definition for RT of GC have been published within the 0116 Intergroup trial [5]. However, these delineations are 2D-based. The CRITICS protocol for 3D-based clinical target volume (CTV) delineation was used for the patients included in this study. This delineation protocol enables a decrease in the inter- and intra-observer variability in the CTV delineation for GC RT [14]. The CTV was delineated individually for all patients, based on information from the diagnostic preoperative CT study, the diagnostic gastroscopy and the postoperative CT images. The CTV consisted of the tumor bed including the gastric remnant, all anastomoses, and up to 16 lymphatic nodes, depending on tumor location and T-stage. The PTV was constructed by adding an isotropic margin of 10 mm to the CTV. The delineated OARs consisted of both kidneys, liver, heart, spinal cord and the part of the bowel that was extending outside of the PTV, encompassed by both the colon and the small intestine (from here on, named bowel).

Treatment planning

The treatment plans were prepared on the postoperative CT image studies. These CT images consisted of 3-mm-thick slices. The prescription dose was 45 Gy (IsoE), delivered in 25 fractions. A generic RBE of 1.1 was assumed for the proton-beam treatment plans. The plans were optimized with the objective of covering 95% of the PTV with at least 95% of the prescription dose. The maximum allowed dose to the PTV was 107% of the prescription dose. The constraints for the OARs used in the treatment planning, together with the values recommended by the quantitative analysis of normal tissue effects in the clinic (QUANTEC), are presented in Supplementary Table 1. No specific constraints were set for the heart, lungs and the bowel. The doses to these OARs were limited as much as possible by avoiding direct irradiations through these OARs. The VMAT plans were used for the clinical treatments of these patients, while the proton plans were retrospectively created for comparison.

The treatment plans were prepared using the Eclipse (Varian Medical Systems, Palo Alto, CA, USA) treatment planning system (TPS). The VMAT plans were prepared using beam data from a 6-MV Varian linear accelerator. The VMAT technique, with two full arcs of 360°, was used. The treatment plans with scanned proton beams were prepared using beam data from an IBA cyclotron (Ion Beam Applications S.A., Louvain-La-Neuve, Belgium) with energies varying between 70 MeV and 235 MeV. A two-field configuration, consisting of an anterior and a lateral field, was used in the proton-beam plans. The lateral field was incident on the left side of the patient. This field configuration was used to produce homogeneous dose coverage of the PTV, while providing adequate sparing of the OARs. Beam setups with only one proton field were disregarded because a too high dose was then given to the bowel. Plans with three fields were also disregarded due to the increased exposures of the liver and the kidneys. The proton plans were optimized using the SFUD method, for which each individual field produces a uniform dose distribution across the target volume. The aim was to achieve a similar or improved PTV dose-coverage, as obtained with the reference VMAT plans, while using the same constraints for the OARs. The dose calculations for the VMAT plans were performed using the analytical anisotropic algorithm (AAA) and the proton convolution superposition (PCS) algorithm was used for the SFUD plans.

Based on the original CT study, two modified CT image sets were created. The aim of creating these sets was to simulate two extreme cases of density fluctuations. In one CT image set, all the gas in the intestines and in the gastric remnant were delineated and given the Hounsfield-unit (HU) value of water. In the other modified CT-image set, the presence of additional gas in the abdomen was simulated by expanding all the bowel- and gastric-gas cavities with 5 mm in all directions. The shapes of the CTV/PTV in the modified CT studies remained the same as outlined in the original CT studies. The volumes of the CTV, PTV as well as the volumes containing extra water- and air-filling in the modified CT image sets are presented in Supplementary Table 2 for all patients.

The original plans were then recalculated on these modified CT image sets, without making any new optimization of the beam fluence. From here on, the CT image sets containing extra water filling will be referred to as water-CT, while the CT sets with expanded air cavity volumes will be referred to as air-CT.

Plan evaluation

For each patient, two comparisons were performed. First of all, the different dose–volume values obtained for the CTV,

PTV and for the OARs with the VMAT- and SFUD-plans, calculated on the original CT studies, were compared. A further comparison was then performed of the dose–volume values obtained when the VMAT and SFUD plans were calculated on the original CT study with the values obtained when the plans were calculated on the modified CT studies.

The relative CTV and PTV volumes encompassed by the 95% isodose surface were determined. In order to evaluate the influence of the fluctuating abdominal gas content on the dose homogeneity in the PTV, the homogeneity index (HI) was calculated for all patients. The equation used for calculating the HI is presented in the Supplementary material. For the OARs, several dose–volume metrics were used for the comparisons: V18 for the kidneys; V10, V30 and mean dose for the liver; V20, V40 and mean dose for the bowel; V25 for the heart and the maximum dose for the spinal cord.

A pairwise comparison of the plans was then performed with a two-sided Wilcoxon signed-rank test with a significance level of .05.

Results

The dose distributions calculated with the VMAT and SFUD plans on the original CT study are shown in Figure 1 for patient #5 and the corresponding DVHs are displayed in Figure 2. The volume of the surrounding normal tissue irradiated was reduced with the SFUD plan, compared to the VMAT plan (Figure 1(a)). A visual comparison of the dose distributions obtained when the plans were recalculated on the water-CT (Figure 1(b)) and air-CT studies (Figure 1(c)) indicated that the SFUD plans were more influenced by the density changes, compared to the corresponding VMAT plans.

A comparison of the original VMAT and SFUD plans

The planning objectives for the PTV were fulfilled for the VMAT- and SFUD-plans prepared and calculated on the original CT studies for all patients (Figure 3). The dose–volume values for the kidneys, liver and spinal cord were reduced in the SFUD plans, compared to the VMAT plans ($p<.05$) (Table 1). The V18 for the right and left kidney decreased with median values of 6% and 26%, respectively. For the liver, there was a decrease in the median values of V10 (66%), V30 (6%) and the mean dose (14.6 Gy (IsoE)). The median decrease in the maximum dose given to the spinal cord was 26.6 Gy (IsoE). However, for the heart, there was a slight increase of V25 with 4% in the SFUD plans ($p\ll.05$).

The impact of the density changes

PTV/CTV coverage

The introduction of density changes caused a deterioration of the PTV/CTV coverage, which was more evident for the SFUD plans (Figure 3 and in Supplementary Table 3). The median value of the PTV dose-coverage in the original SFUD plans was 99%. It decreased to 87% for the plans recalculated on the water-CT sets and to 86% for the plans recalculated on the air-CT sets. The loss of CTV dose-coverage was also observed in the SFUD plans prepared on modified CT sets (Supplementary Table 3). Median values of the HI of 0.07 (0.05–0.11), 0.08 (0.06–0.17) and 0.11 (0.09–0.17) were obtained for the VMAT plans calculated on the original CT studies, the water-CT studies and the air-CT studies, respectively. In the SFUD plans, the median values of the HIs were 0.07 (0.06–0.18) for the original plans, 0.29 (0.08–0.51) for the plans recalculated on the water-CT sets and 0.14 (0.09–0.25) for the plans recalculated on the air-CT sets.

Sparing of the OARs

In the VMAT plans, there was no significant difference in the dose–volume values registered for the OARs in the plans calculated on the modified CT sets, compared to the original VMAT plans ($p>.05$), except for the liver mean dose, which

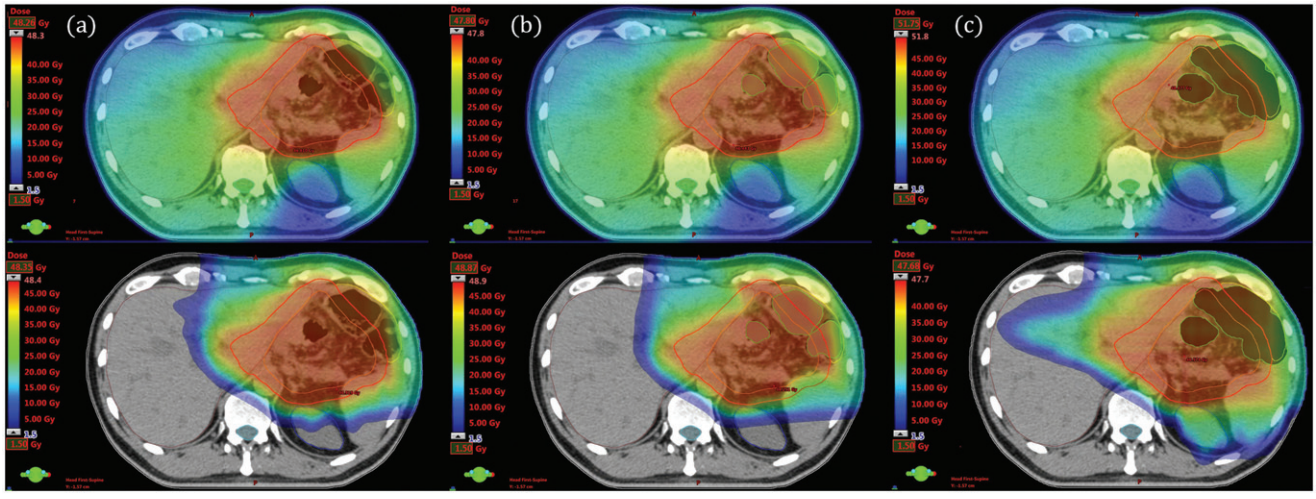

Figure 1. Dose distributions calculated in the axial plane of GC patient # 5, planned with photon-beam based VMAT (top) and with proton-beam based SFUD (bottom) on (a) the original CT image set, (b) a modified CT set with water filling (water-CT) and (c) a modified CT set with expanded volumes of the abdominal air-cavities (air-CT). The contours of the PTV (red), CTV (orange), liver (brown), right kidney (blue), spinal cord (light blue) and bowel (yellow) are also visualized in this slice. In (b) and (c), the artificial structures containing water- or air-equivalent material are contoured in green and contain gray or black filling, respectively. Proton doses are presented in Gy (IsoE).

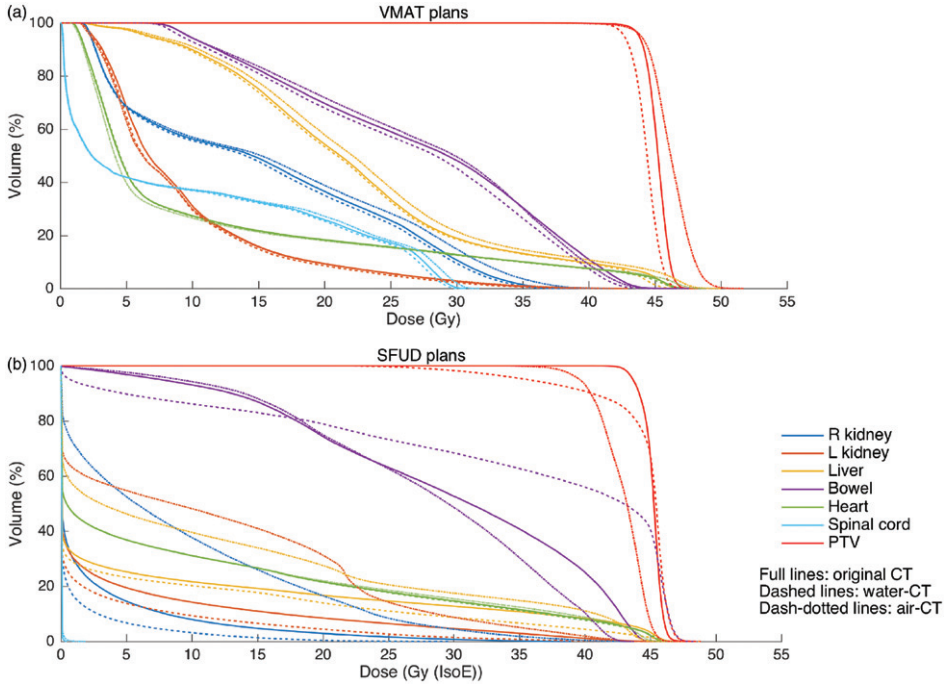

Figure 2. Dose–volume histograms for patient # 5 planned with VMAT (a) and with SFUD (b). The plans were prepared on the original CT image study (full lines), and recalculated on the CT set with additional water filling (dashed lines) and on the CT set with expanded air volume (dotted lines).

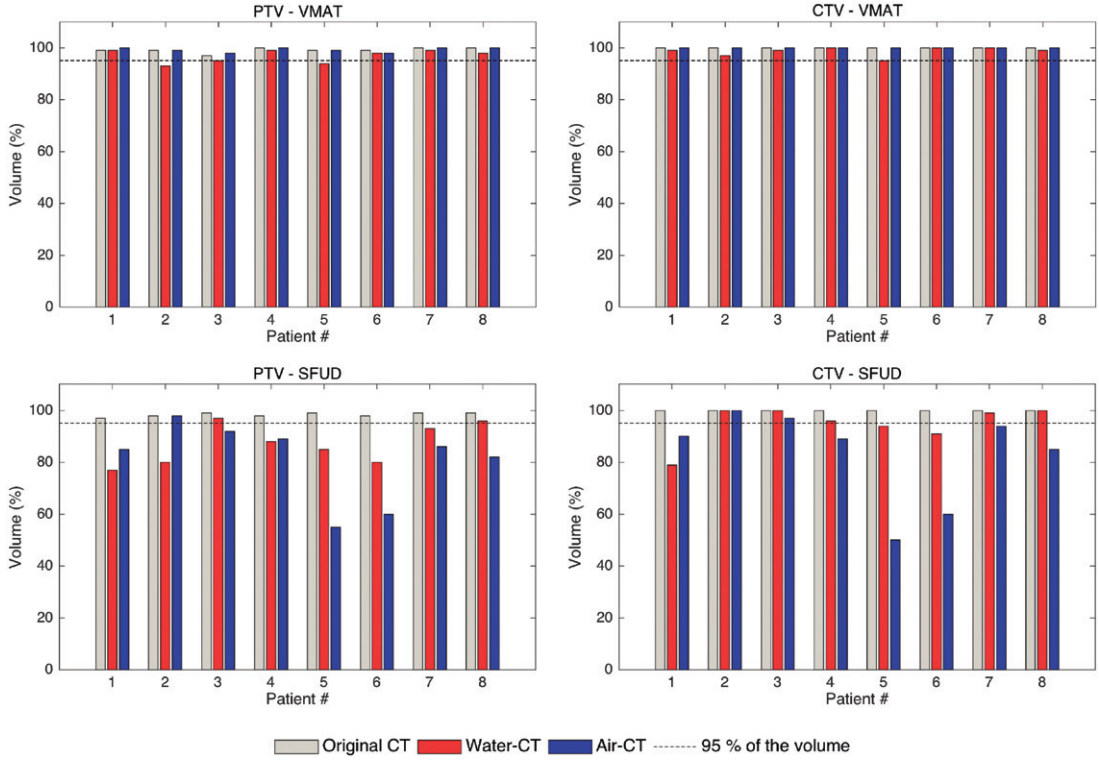

Figure 3. The fractional volumes of the PTV and CTV encompassed by the 95% isodose surface in the VMAT and SFUD plans prepared on the original CT image sets and recalculated on the modified CT sets with extra water filling and with expanded volumes of the abdominal air-cavities.

decreased slightly in the VMAT plans calculated on the water-CT sets ($p<.05$) (Table 1).

In the SFUD plans calculated on the water-CT sets, there was a slight decrease of the median dose–volume values for the left kidney, liver and bowel (V20 and mean dose) ($p<.05$) (Table 1). On the other hand, the expansion of the air volumes caused increases in the values of V18 for the right (10%) and the left kidneys (12%) compared to the original SFUD-plans ($p<.05$) (Table 1). The three metrics for the liver increased with median values of 12% (V10), 3% (V30) and

Table 1. The median values (range) of the differences between the dose–volume values obtained for the OARs in the original plans and those obtained in plans using the modified CT studies are shown. The median values (range) of the differences between the dose–volume values obtained for the OARs in the original VMAT- and SFUD-plans are also presented. The p values obtained from the statistical test performed are also shown.

		VMAT		SFUD		Original plans
OARs	Dose–volume metric	(Original) − (Water-CT)	(Original) − (Air-CT)	(Original) − (Water-CT)	(Original) − (Air-CT)	(VMAT − SFUD)
Right kidney	V18 (%)	0 (−1 to 3)	−1 (−2 to 2)	0 (0 to 3)	−10 (−29 to 0)[a]	6 (−1 to 38)[a]
Left kidney	V18 (%)	0 (−14 to 9)	0 (−16 to 8)	4 (0 to 14)[b]	−12 (−45 to 0)[b]	26 (2 to 55)[b]
Both kidneys	V18 (%)	0 (−1 to 15)	0 (−2 to 15)	1 (−2 to 8)	−8 (−38 to 0)[b]	21 (1 to 33)[b]
Liver	V10 (%)	0 (0 to 4)	0 (−1 to 3)	1 (0 to 4)[b]	−12 (−20 to 0)[b]	66 (59 to 73)[b]
	V30 (%)	0 (−1 to 7)	−1 (−3 to 5)	2 (0 to 5)[b]	−3 (−5 to 0)[b]	6 (2 to 20)[b]
	D_{mean} Gy (IsoE)	0.2 (0.0 to 3.0)[a]	−0.3 (−4.0 to 2.2)	0.7 (0.0 to 1.9)[b]	−3.2 (−4.9 to 0.0)[b]	14.6 (10.6 to 65.1)[b]
Bowel	V20 (%)	1 (0 to 5)	−2 (−6 to 3)	1 (0 to 4)[a]	−1 (−9 to 3)	16 (−11 to 31)
	V40 (%)	1 (−1 to 16)	−2 (−3 to 14)	0 (−1 to 8)	4 (0 to 23)[a]	−5 (−19 to 16)
	D_{mean} Gy (IsoE)	0.3 (−0.2 to 4.4)	−0.7 (−1.4 to 3.5)	0.3 (−0.2 to 1.2)[a]	0.0 (−3.5 to 1.9)	3.9 (−3.1 to 9.1)
Heart	V25 (%)	0 (0 to 2)	0 (−1 to 2)	0 (0 to 0)	0 (−2 to 0)	−4 (−13 to (−1))[b]
Spinal cord	D_{max} Gy (IsoE)	0.3 (−0.5 to 4.4)	−0.2 (−1.3 to 18.5)	0.0 (−0.8 to 3.6)	−3.4 (−23.4 to 0.0)	26.6 (11.4 to 33.6)[b]

[a]$p<.05$; [b]$p\ll.05$; otherwise $p>.05$.

3.2 Gy (IsoE) (mean dose) ($p \ll .05$) (Table 1). For the bowel, there was also an increase in the V40 (4%) in the SFUD plans calculated on air-CT sets ($p < .05$) (Table 1).

The absolute values of the different dose–volume metrics obtained for all the OARs are illustrated in Figure 4 and presented in Supplementary Table 4.

Discussion

The improved normal-tissue sparing achievable with proton beams, in the treatment of large abdominal targets, has been described in several reports [4,11,12,15]. In this work, we found that the SFUD plans, calculated on the original CT image sets, provided better or comparable sparing of the OARs, compared to the VMAT plans. However, the VMAT plans were found to be more robust against the introduced density changes. The dose–volume values determined for the PTV and OARs were similar when the VMAT plans were calculated on the three distinct CT sets. On the other hand, the proton range is strongly dependent on the density of the traversed medium. Therefore, the SFUD plans were more influenced by the introduced density changes (Figures 3 and 4). In the SFUD plans calculated on the water-CT studies, there was a shift of the position of the high-dose volumes toward the proximal surface of the PTV, resulting in an under dosage toward the distal part of the PTV. When instead extra air volumes were added in the abdomen, the high-dose volumes were shifted toward the dorsal/right part of the abdomen, which resulted in under dosage of the proximal part of the PTV combined with higher doses given to the right kidney and the liver. The magnitude of the changes in the dose distributions was depending on the initial volume of the gastrointestinal gas and its location in relation to the proton beams (Figure 1). The change was larger for patients with larger air-cavity volumes (Supplementary Table 2). Despite the fact that the variations in the gastrointestinal gas volumes resulted in altered dose distributions in the OARs, the density variations did not result in doses exceeding the pre-set dose–volume constraints for the OARs.

The density variations produced cold spots in the PTVs in the dose distributions calculated with the SFUD plans, both in the proximal and distal regions of the target. The distortion of the dose distributions can be expected to be even more severe when intensity modulated proton therapy is used [16], due to the shape of the dose-distribution produced by each single beam.

The degradation of the dose distribution due to density changes can also be observed to a certain extent in the VMAT plans in the form of cold- and/or hot-spots in the PTV (see Figure 2(a)). In photon-RT, the uncertainties related to physiological changes within the patient are generally accounted for by using internal margins around the CTV, as suggested in the ICRU Report 62 [17]. For PBT, this strategy is not sufficient to keep this type of uncertainties under control. In the ICRU Report 78 [18], the use of proximal and distal field-specific margins is recommended, in addition to the lateral margins used during PTV delineation, to account for the proton-beam specific range uncertainties. These field-specific margins could be adapted to account also for the inter-fraction variation of the densities of the surrounding tissues and the target filling [16]. However, this may imply that larger volumes of the surrounding healthy tissue are irradiated. The range uncertainty in PBT is an even larger issue in the presence of fluctuating tissue densities [19,20]. Thus, approaches for mitigating the tissue-density uncertainties in PBT of tumors influenced by density changes are needed. Such approaches include the use of image-guided radiation therapy (IGRT) [21].

The optimal beam-configuration in PBT of GC has still not been determined due to the uncertainties related to density changes in the irradiation field. Historically, the photon treatments of GC have been performed using the traditional anteriorposterior–posterioranterior (AP–PA) field configuration. Different studies have shown that this setup is inferior to other techniques used in modern photon-based RT, e.g., 3D-CRT, IMRT, VMAT regarding the sparing of the OARs and the PTV coverage [22,23]. In most of the previous studies of PBT of GC, a setup with a dorsal field, or a field passing through the liver [4], have been utilized in order to minimize the deteriorating effects of the density variations. However, this approach also reduces the potential advantage of PBT since the proton fields will then pass through important OARs, e.g.,

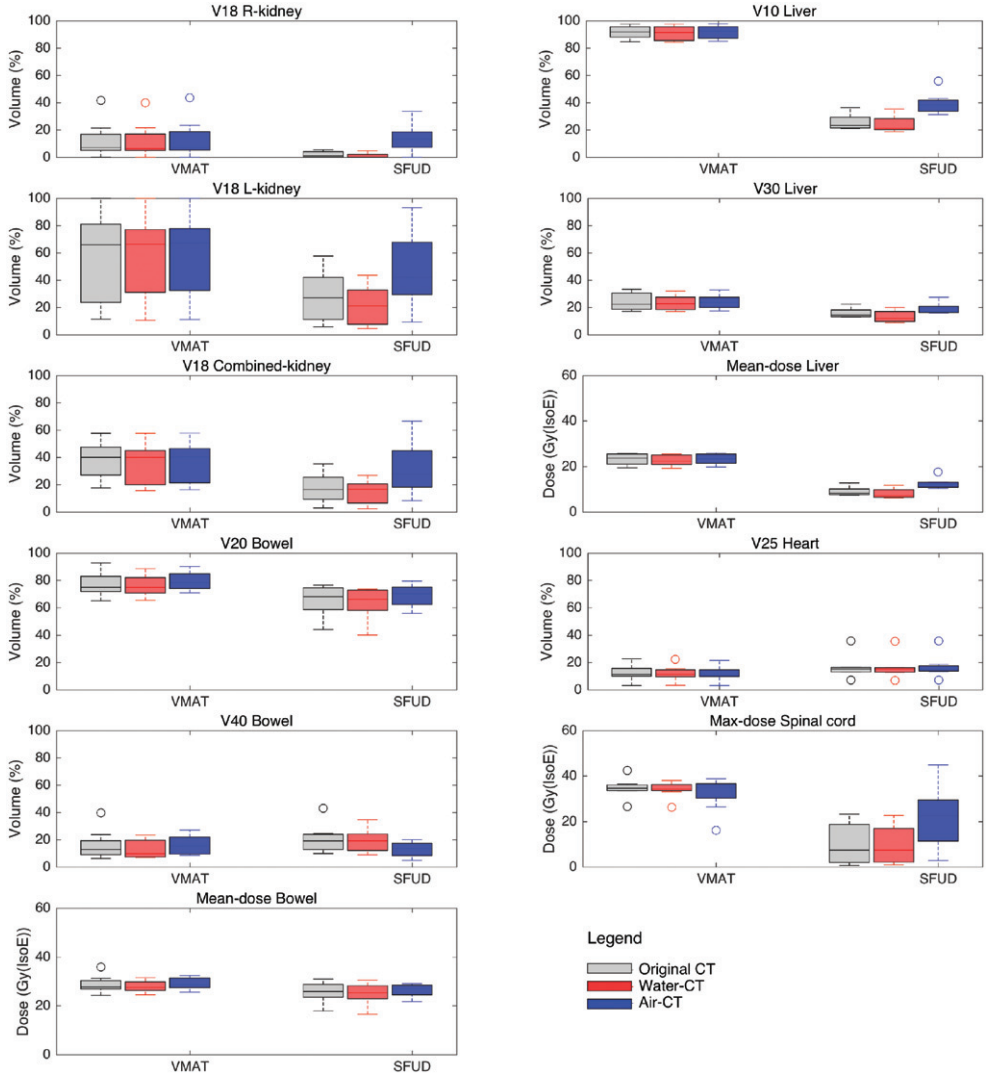

Figure 4. Box plot (presenting the median, minimum and maximum values together with the first and third quartile) showing the dose–volume values obtained for all the OARs with the VMAT and SFUD treatment plans. The plans have been calculated on the original CT image sets and recalculated on the modified CT image sets.

the spinal cord, the liver and the kidneys. Dionisi et al. [4] reported a better sparing of the OARs when using passive-scattering proton beams, compared to IMRT. A posterior-lateral field configuration was used in their work. A frontal field was added for some cases to improve the target dose-coverage. In the present study, the field configuration used in the SFUD plans was selected to provide optimal PTV coverage and sparing of the OARs, without considering potential density variations along the beam path. This setup was selected because the main aim of this work was to quantify the impact of the density variations in worst-case scenarios.

The advantage of PBT is mostly related to the reductions of the low and intermediate doses given to large volumes of the OARs which are located close to the PTV [24]. In the current study, the OARs which were closest to the PTV (with some parts overlapping) were the bowel and the heart. No dose–volume constraints were set for these two organs in the treatment planning. The threshold value for observing long-term cardiac mortality after RT was exceeded in both the VMAT and SFUD plans, calculated on the original CT studies (Supplementary Table 4). On the other hand, the bowel is the dose limiting OAR in the RT of GC, due to the elevated risk of radiation-induced bowel obstruction. QUANTEC sets a threshold value of $V45 < 195\,cm^3$ for the small bowel (Supplementary Table 1). However, in this study, the bowel was delineated as both the small and large intestines. The V45 was below this threshold for all patients. Other critical structures, for which dose–volume constraints were set during the treatment planning, were the right kidney, liver and spinal cord. For these OARs, the threshold values set by QUANTEC (Supplementary Table 1) were not exceeded in the original VMAT plans, except for patient # 5, for which the left, instead of the right kidney was spared. The dose–volume constraints were also respected in the VMAT plans recalculated on the modified CT studies. In the original SFUD plans, the dose–volume values registered for these OARs were reduced, compared with the VMAT plans. In the SFUD plans calculated on the air-CT image sets, the dose–volume values obtained

for these three OARs were higher, but still below the threshold values set by QUANTEC.

In the present study, the influence of density changes on the dose distributions produced by the VMAT and SFUD plans were studied by manipulating the HUs in the planning CT studies. However, this method does not simulate in detail all the intra- and inter-fraction variations in shape, position and contents of the PTV and the OARs which would be necessary to provide a more complete description of the impact of the tissue density changes on the produced dose distributions. The inter-fraction density changes make the dose distributions deviate from those obtained for the planning CT studies. Nevertheless, the sometimes rapid fluctuations in the dose distribution, obtained for a particular fraction, can be expected to be averaged out during a full course of RT. The use of imaging during the treatment course could provide patient-specific information of the density changes that could be used for evaluating their impact on the resulting dose distributions [25].

In conclusion, the results obtained in this study showed that, in a static setting, the SFUD technique can be used to reduce the doses given to OARs in the adjuvant treatment of GC. However, the SFUD plans were found to be less robust against larger density changes, compared to the VMAT plans, which led to inferior treatments for such cases. Therefore, adaptive approaches, which can mitigate the impact of large density variations, are needed in PBT of GC.

Funding

This study was financially supported by the Swedish International Development Corporation (SIDA) through the International Science Programme (ISP) at Uppsala University and the Cancer Research Funds of Radiumhemmet at Karolinska Institute.

Disclosure statement

The authors report no conflicts of interest. The authors alone are responsible for the content and writing of this article.

References

[1] Ferlay J, Soerjomataram I, Dikshit R, et al. Cancer incidence and mortality worldwide: sources, methods and major patterns in GLOBOCAN 2012. Int J Cancer. 2015;136:E359–E386.
[2] Dupont JB, Lee JR, Burton GR, et al. Adenocarcinoma of the stomach: review of 1,497 cases. Cancer. 1978;41:941–947.
[3] Shi Y, Zhou Y. The role of surgery in the treatment of gastric cancer. J Surg Oncol. 2010;101:687–692.
[4] Dionisi F, Amichetti M, Avery S, et al. Proton therapy in adjuvant treatment of gastric cancer: planning comparison with advanced X-ray therapy and feasibility report. Acta Oncol (Madr). 2014;53:1312–1320.
[5] Macdonald JS, Smalley SR, Benedetti J, et al. Chemoradiotherapy after surgery compared with surgery alone for adenocarcinoma of the stomach or gastroesophageal junction. N Engl J Med. 2001; 345:725–730.
[6] Cunningham D, Allum WH, Stenning SP, et al. Perioperative chemotherapy versus surgery alone for resectable gastroesophageal cancer. N Engl J Med. 2006;355:11–20.
[7] Coburn NG, Guller U, Baxter NN, et al. Adjuvant therapy for resected gastric cancer-rapid, yet incomplete adoption following results of intergroup 0116 trial. Int J Radiat Oncol Biol Phys. 2008;70:1073–1080.
[8] Dikken JL, van Sandick JW, Maurits Swellengrebel HA, et al. Neoadjuvant chemotherapy followed by surgery and chemotherapy or by surgery and chemoradiotherapy for patients with resectable gastric cancer (CRITICS). BMC Cancer. 2011;11:329.
[9] Kozak KR, Kachnic LA, Adams J, et al. Dosimetric feasibility of hypofractionated proton radiotherapy for neoadjuvant pancreatic cancer treatment. Int J Radiat Oncol Biol Phys. 2007; 68:1557–1566.
[10] Nichols RC, George TJ, Zaiden RA, et al. Proton therapy with concomitant capecitabine for pancreatic and ampullary cancers is associated with a low incidence of gastrointestinal toxicity. Acta Oncol. 2013;52:498–505.
[11] Nichols RC, Huh SN, Prado KL, et al. Protons offer reduced normal-tissue exposure for patients receiving postoperative radiotherapy for resected pancreatic head cancer. Int J Radiat Oncol Biol Phys. 2012;83:158–163.
[12] Radu C, Norrlid O, Brndengen M, et al. Integrated peripheral boost in preoperative radiotherapy for the locally most advanced non-resectable rectal cancer patients. Acta Oncol. 2013;52: 528–537.
[13] Zhang X, Zhao K-L, Guerrero TM, et al. Four-dimensional computed tomography-based treatment planning for intensity-modulated radiation therapy and proton therapy for distal esophageal cancer. Int J Radiat Oncol Biol Phys. 2008;72: 278–287.
[14] Jansen EPM, Nijkamp J, Gubanski M, et al. Interobserver variation of clinical target volume delineation in gastric cancer. Int J Radiat Oncol Biol Phys. 2010;77:1166–1170.
[15] Nichols RC, Huh SH, Hoppe BS, et al. Protons safely allow coverage of high-risk nodes for patients with regionally advanced non-small-cell lung cancer. Technol Cancer Res Treat. 2011; 10:317–322.
[16] Engelsman M, Bert C. Precision and uncertainties in proton therapy of moving targets. In: Paganetti H, editor. Proton therapy physics. Boca Raton (FL): CRC Press; 2012. p. 435–460.
[17] International Commission on Radiation Units and Measurements. ICRU Report 62. Prescribing, Recording, and Reporting Photon Beam Therapy (Supplement to ICRU Report 50). J ICRU. Bethesda, Maryland; 1999.
[18] International Commission on Radiation Units and Measurements. ICRU Report 78: prescribing, Recording and Reporting Photon Beam Therapy. Oxford University Press; 2007.
[19] Lomax AJ. Intensity modulated proton therapy and its sensitivity to treatment uncertainties 1: the potential effects of calculational uncertainties. Phys Med Biol. 2008;53:1027–1042.
[20] Sawakuchi GO, Titt U, Mirkovic D, et al. Density heterogeneities and the influence of multiple coulomb and nuclear scatterings on the Bragg peak distal edge of proton therapy beams. Phys Med Biol. 2008;53:4605–4619.
[21] Jaffray DA. Image-guided radiotherapy: from current concept to future perspectives. Nat Rev Clin Oncol. 2012;9:688–699.
[22] Wieland P, Dobler B, Mai S, et al. IMRT for postoperative treatment of gastric cancer: covering large target volumes in the upper abdomen: a comparison of a step-and-shoot and an arc therapy approach. Int J Radiat Oncol Biol Phys. 2004; 59:1236–1244.
[23] Wang X, Li G, Zhang Y, et al. Single-arc volumetric-modulated arc therapy (sVMAT) as adjuvant treatment for gastric cancer: dosimetric comparisons with three-dimensional conformal radiotherapy (3D-CRT) and intensity-modulated radiotherapy (IMRT). Med Dosim. 2013;38:395–400.
[24] Mondlane G, Gubanski M, Lind P, et al. Dosimetric comparison of plans for photon- or proton-beam based radiosurgery of liver metastases. Int J Part Ther. 2016;3:277–284.
[25] Hui Z, Zhang X, Starkschall G, et al. Effects of interfractional motion and anatomic changes on proton therapy dose distribution in lung cancer. Int J Radiat Oncol Biol Phys. 2008;72:1385–1395.